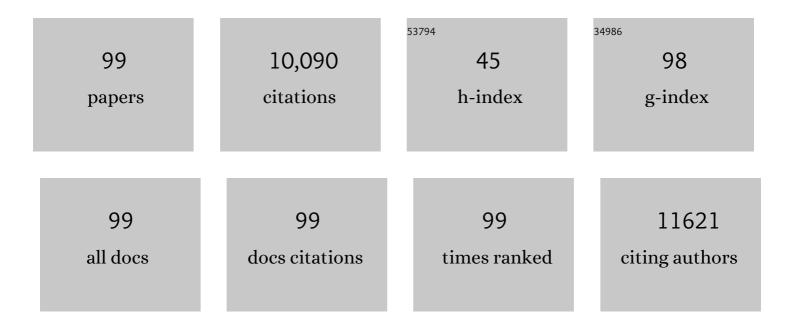
List of Publications by Year in descending order

Source: https://exaly.com/author-pdf/6225880/publications.pdf Version: 2024-02-01



Μει Ζησι

#	Article	IF	CITATIONS
1	Emerging Multifunctional Metal–Organic Framework Materials. Advanced Materials, 2016, 28, 8819-8860.	21.0	1,227
2	Unveiling the Activity Origin of a Copperâ€based Electrocatalyst for Selective Nitrate Reduction to Ammonia. Angewandte Chemie - International Edition, 2020, 59, 5350-5354.	13.8	760
3	Recent Progress in Metalâ€Organic Frameworks for Applications in Electrocatalytic and Photocatalytic Water Splitting. Advanced Science, 2017, 4, 1600371.	11.2	594
4	In Situ Bond Modulation of Graphitic Carbon Nitride to Construct p–n Homojunctions for Enhanced Photocatalytic Hydrogen Production. Advanced Functional Materials, 2016, 26, 6822-6829.	14.9	583
5	Dynamic traction of lattice-confined platinum atoms into mesoporous carbon matrix for hydrogen evolution reaction. Science Advances, 2018, 4, eaao6657.	10.3	460
6	Synthesis of Particulate Hierarchical Tandem Heterojunctions toward Optimized Photocatalytic Hydrogen Production. Advanced Materials, 2018, 30, e1804282.	21.0	411
7	Photoassisted Construction of Holey Defective gâ€C ₃ N ₄ Photocatalysts for Efficient Visibleâ€Lightâ€Driven H ₂ O ₂ Production. Small, 2018, 14, 1703142.	10.0	353
8	Surface Modulation of Hierarchical MoS ₂ Nanosheets by Ni Single Atoms for Enhanced Electrocatalytic Hydrogen Evolution. Advanced Functional Materials, 2018, 28, 1807086.	14.9	314
9	Unveiling the Promotion of Surfaceâ€Adsorbed Chalcogenate on the Electrocatalytic Oxygen Evolution Reaction. Angewandte Chemie - International Edition, 2020, 59, 22470-22474.	13.8	257
10	Direct and Selective Photocatalytic Oxidation of CH ₄ to Oxygenates with O ₂ on Cocatalysts/ZnO at Room Temperature in Water. Journal of the American Chemical Society, 2019, 141, 20507-20515.	13.7	253
11	Intramolecular electronic coupling in porous iron cobalt (oxy)phosphide nanoboxes enhances the electrocatalytic activity for oxygen evolution. Energy and Environmental Science, 2019, 12, 3348-3355.	30.8	234
12	A modular strategy for decorating isolated cobalt atoms into multichannel carbon matrix for electrocatalytic oxygen reduction. Energy and Environmental Science, 2018, 11, 1980-1984.	30.8	225
13	Oxygen vacancies induced special CO2 adsorption modes on Bi2MoO6 for highly selective conversion to CH4. Applied Catalysis B: Environmental, 2019, 259, 118088.	20.2	221
14	Isolated Cobalt Centers on W ₁₈ O ₄₉ Nanowires Perform as a Reaction Switch for Efficient CO ₂ Photoreduction. Journal of the American Chemical Society, 2021, 143, 2173-2177.	13.7	199
15	Hierarchical MoS ₂ Hollow Architectures with Abundant Mo Vacancies for Efficient Sodium Storage. ACS Nano, 2019, 13, 5533-5540.	14.6	187
16	Anion Etching for Accessing Rapid and Deep Self-Reconstruction of Precatalysts for Water Oxidation. Matter, 2020, 3, 2124-2137.	10.0	177
17	Cubic quantum dot/hexagonal microsphere ZnIn ₂ S ₄ heterophase junctions for exceptional visible-light-driven photocatalytic H ₂ evolution. Journal of Materials Chemistry A, 2017, 5, 8451-8460.	10.3	176
18	Implanting Isolated Ru Atoms into Edgeâ€Rich Carbon Matrix for Efficient Electrocatalytic Hydrogen Evolution. Advanced Energy Materials, 2020, 10, 2000882.	19.5	144

#	Article	IF	CITATIONS
19	Constructing Conductive Interfaces between Nickel Oxide Nanocrystals and Polymer Carbon Nitride for Efficient Electrocatalytic Oxygen Evolution Reaction. Advanced Functional Materials, 2019, 29, 1904020.	14.9	140
20	Hydrogen-Intercalation-Induced Lattice Expansion of Pd@Pt Core–Shell Nanoparticles for Highly Efficient Electrocatalytic Alcohol Oxidation. Journal of the American Chemical Society, 2021, 143, 11262-11270.	13.7	121
21	Selective Photo-oxidation of Methane to Methanol with Oxygen over Dual-Cocatalyst-Modified Titanium Dioxide. ACS Catalysis, 2020, 10, 14318-14326.	11.2	114
22	Improved charge separation and surface activation via boron-doped layered polyhedron SrTiO3 for co-catalyst free photocatalytic CO2 conversion. Applied Catalysis B: Environmental, 2017, 219, 10-17.	20.2	113
23	Rational design of freestanding MoS2 monolayers for hydrogen evolution reaction. Nano Energy, 2017, 39, 409-417.	16.0	107
24	Superficial Hydroxyl and Amino Groups Synergistically Active Polymeric Carbon Nitride for CO ₂ Electroreduction. ACS Catalysis, 2019, 9, 10983-10989.	11.2	105
25	Cation Vacancy-Initiated CO ₂ Photoreduction over ZnS for Efficient Formate Production. ACS Energy Letters, 2019, 4, 1387-1393.	17.4	102
26	Band gap engineering of bulk and nanosheet SnO: an insight into the interlayer Sn–Sn lone pair interactions. Physical Chemistry Chemical Physics, 2015, 17, 17816-17820.	2.8	100
27	Ultrathin FeOOH nanosheets as an efficient cocatalyst for photocatalytic water oxidation. Journal of Materials Chemistry A, 2019, 7, 9222-9229.	10.3	100
28	Synthesis of a Boron–Imidazolate Framework Nanosheet with Dimer Copper Units for CO ₂ Electroreduction to Ethylene. Angewandte Chemie - International Edition, 2021, 60, 16687-16692.	13.8	99
29	n-type boron phosphide as a highly stable, metal-free, visible-light-active photocatalyst for hydrogen evolution. Nano Energy, 2016, 28, 158-163.	16.0	94
30	Powder exfoliated MoS ₂ nanosheets with highly monolayer-rich structures as high-performance lithium-/sodium-ion-battery electrodes. Nanoscale, 2019, 11, 1887-1900.	5.6	93
31	Doping β-CoMoO ₄ Nanoplates with Phosphorus for Efficient Hydrogen Evolution Reaction in Alkaline Media. ACS Applied Materials & Interfaces, 2018, 10, 37038-37045.	8.0	81
32	Periodically Ordered Nanoporous Perovskite Photoelectrode for Efficient Photoelectrochemical Water Splitting. ACS Nano, 2018, 12, 6335-6342.	14.6	74
33	Efficient photocatalytic CO2 reduction over Co(II) species modified CdS in aqueous solution. Applied Catalysis B: Environmental, 2018, 226, 252-257.	20.2	70
34	Engineering the crystallinity of MoS ₂ monolayers for highly efficient solar hydrogen production. Journal of Materials Chemistry A, 2017, 5, 8591-8598.	10.3	69
35	Barium disilicide as a promising thin-film photovoltaic absorber: structural, electronic, and defect properties. Journal of Materials Chemistry A, 2017, 5, 25293-25302.	10.3	68
36	Interface engineered <i>in situ</i> anchoring of Co ₉ S ₈ nanoparticles into a multiple doped carbon matrix: highly efficient zinc–air batteries. Nanoscale, 2018, 10, 2649-2657.	5.6	66

#	Article	IF	CITATIONS
37	A rapidly room-temperature-synthesized Cd/ZnS:Cu nanocrystal photocatalyst for highly efficient solar-light-powered CO2 reduction. Applied Catalysis B: Environmental, 2018, 237, 68-73.	20.2	65
38	Integrated selective nitrite reduction to ammonia with tetrahydroisoquinoline semi-dehydrogenation over a vacancy-rich Ni bifunctional electrode. Journal of Materials Chemistry A, 2021, 9, 239-243.	10.3	65
39	Boron enhances oxygen evolution reaction activity over Ni foam-supported iron boride nanowires. Journal of Materials Chemistry A, 2020, 8, 13638-13645.	10.3	61
40	Unravelling unsaturated edge S in amorphous NiSx for boosting photocatalytic H2 evolution of metastable phase CdS confined inside hydrophilic beads. Applied Catalysis B: Environmental, 2022, 305, 121055.	20.2	58
41	Ultrathin graphene encapsulated Cu nanoparticles: A highly stable and efficient catalyst for photocatalytic H2 evolution and degradation of isopropanol. Chemical Engineering Journal, 2020, 390, 124558.	12.7	55
42	High performance Au–Cu alloy for enhanced visible-light water splitting driven by coinage metals. Chemical Communications, 2016, 52, 4694-4697.	4.1	54
43	Spontaneous Direct Band Gap, High Hole Mobility, and Huge Exciton Energy in Atomic-Thin TiO ₂ Nanosheet. Chemistry of Materials, 2018, 30, 6449-6457.	6.7	50
44	Probing the role of nickel dopant in aqueous colloidal ZnS nanocrystals for efficient solar-driven CO2 reduction. Applied Catalysis B: Environmental, 2019, 244, 1013-1020.	20.2	50
45	Nitrogen-doped ultrathin graphene encapsulated Cu nanoparticles decorated on SrTiO3 as an efficient water oxidation photocatalyst with activity comparable to BiVO4 under visible-light irradiation. Applied Catalysis B: Environmental, 2020, 279, 119352.	20.2	47
46	Fumaric Acid Assistant Band Structure Tunable Nitrogen Defective g-C ₃ N ₄ Fabrication for Enhanced Photocatalytic Hydrogen Evolution. ACS Sustainable Chemistry and Engineering, 2021, 9, 7529-7540.	6.7	47
47	Construction of Porous Co ₉ S ₈ Hollow Boxes with Double Open Ends toward High-Performance Half/Full Sodium-Ion Batteries. ACS Sustainable Chemistry and Engineering, 2020, 8, 6305-6314.	6.7	46
48	Hittorf's violet phosphorene as a promising candidate for optoelectronic and photocatalytic applications: first-principles characterization. Physical Chemistry Chemical Physics, 2018, 20, 11967-11975.	2.8	45
49	Selectivity Origin of Organic Electrosynthesis Controlled by Electrode Materials: A Case Study on Pinacols. ACS Catalysis, 2021, 11, 8958-8967.	11.2	45
50	Dissolution of the Heteroatom Dopants and Formation of Ortho-Quinone Moieties in the Doped Carbon Materials during Water Electrooxidation. Journal of the American Chemical Society, 2022, 144, 3250-3258.	13.7	45
51	Open hollow Co–Pt clusters embedded in carbon nanoflake arrays for highly efficient alkaline water splitting. Journal of Materials Chemistry A, 2018, 6, 20214-20223.	10.3	42
52	Stabilizing CuGaS ₂ by crystalline CdS through an interfacial Z-scheme charge transfer for enhanced photocatalytic CO ₂ reduction under visible light. Nanoscale, 2020, 12, 8693-8700.	5.6	39
53	Visible light driven hydrogen evolution using external and confined CdS: Effect of chitosan on carriers separation. Applied Catalysis B: Environmental, 2020, 277, 119152.	20.2	39
54	Tailoring Band Structure of TiO ₂ To Enhance Photoelectrochemical Activity by Codoping S and Mg. Journal of Physical Chemistry C, 2015, 119, 11557-11562.	3.1	34

#	Article	IF	CITATIONS
55	Tunable Photocatalytic HER Activity of Single-Layered TiO ₂ Nanosheets with Transition-Metal Doping and Biaxial Strain. Journal of Physical Chemistry C, 2019, 123, 526-533.	3.1	34
56	Scaling law of hydrogen evolution reaction for InSe monolayer with 3d transition metals doping and strain engineering. Journal of Energy Chemistry, 2020, 41, 107-114.	12.9	34
57	Pulsed electrocatalysis enables the stabilization and activation of carbon-based catalysts towards H2O2 production. Applied Catalysis B: Environmental, 2022, 316, 121688.	20.2	32
58	Amorphous molybdenum sulfide mediated EDTA with multiple active sites to boost heavy metal ions removal. Chinese Chemical Letters, 2021, 32, 2797-2802.	9.0	31
59	Construction of a 3D/2D g-C ₃ N ₄ /ZnIn ₂ S ₄ hollow spherical heterostructure for efficient CO ₂ photoreduction under visible light. Catalysis Science and Technology, 2021, 11, 1282-1291.	4.1	28
60	Sulfur-Doped Flowerlike Porous Carbon Derived from Metal–Organic Frameworks as a High-Performance Potassium-Ion Battery Anode. ACS Applied Energy Materials, 2021, 4, 2282-2291.	5.1	28
61	Enhanced adsorption of Cr(<scp>vi</scp>) on BiOBr under alkaline conditions: interlayer anion exchange. Environmental Science: Nano, 2019, 6, 3601-3610.	4.3	27
62	Activated HER performance of defected single layered TiO2 nanosheet via transition metal doping. International Journal of Hydrogen Energy, 2020, 45, 2681-2688.	7.1	27
63	Tunable electronic and magnetic properties of antimonene system via Fe doping and defect complex: A first-principles perspective. Applied Surface Science, 2018, 448, 281-287.	6.1	24
64	Enhanced Visible-Light-Driven Hydrogen Production of Carbon Nitride by Band Structure Tuning. Journal of Physical Chemistry C, 2018, 122, 17261-17267.	3.1	23
65	Efficient photocatalytic CO ₂ reduction mediated by transitional metal borides: metal site-dependent activity and selectivity. Journal of Materials Chemistry A, 2020, 8, 21833-21841.	10.3	23
66	Superionic conduction along ordered hydroxyl networks in molecular-thin nanosheets. Materials Horizons, 2019, 6, 2087-2093.	12.2	22
67	Built-In Electric Field Hindering Photogenerated Carrier Recombination in Polar Bilayer SnO/BiOX (X =) Tj ETQq1	1 0,784314 3.1	1 rgBT /Overl
68	Lithium doped nickel oxide nanocrystals with a tuned electronic structure for oxygen evolution reaction. Chemical Communications, 2021, 57, 6070-6073.	4.1	22
69	Rational Design of a High-Durability Pt-Based ORR Catalyst Supported on Mn/N Codoped Carbon Sheets for PEMFCs. Energy & Fuels, 2022, 36, 1707-1715.	5.1	22
70	Single-atom catalysts for thermal- and electro-catalytic hydrogenation reactions. Journal of Materials Chemistry A, 2022, 10, 5743-5757.	10.3	22
71	Hydrated electrons mediated in-situ construction of cubic phase CdS/Cd thin layer on a millimeter-scale support for photocatalytic hydrogen evolution. Journal of Colloid and Interface Science, 2022, 607, 769-781.	9.4	20
72	Tridecaboron diphosphide: a new infrared light active photocatalyst for efficient CO ₂ photoreduction under mild reaction conditions. Journal of Materials Chemistry A, 2021, 9, 2421-2428.	10.3	19

#	Article	IF	CITATIONS
73	Novel optical and magnetic properties of Li-doped quasi-2D manganate Ca ₃ Mn ₂ O ₇ particles. Journal of Materials Chemistry C, 2017, 5, 7011-7019.	5.5	18
74	Improved photocatalytic HER activity of α-Sb monolayer with doping and strain engineering. Applied Surface Science, 2020, 507, 145194.	6.1	17
75	Enhanced Lubrication and Photocatalytic Degradation of Liquid Paraffin by Hollow MoS ₂ Microspheres. ACS Omega, 2018, 3, 3120-3128.	3.5	14
76	Tunable HER activity from doping and strain strategies for β-Sb monolayer: DFT calculations. Computational Materials Science, 2020, 185, 109966.	3.0	14
77	Fabrication of Ultrathin Two-Dimensional/Two-Dimensional MoS ₂ /ZnIn ₂ S ₄ Hybrid Nanosheets for Highly Efficient Visible-Light-Driven Photocatalytic Hydrogen Evolution. ACS Applied Energy Materials, 2022, 5, 8232-8240.	5.1	14
78	Computational Design of Copper doped Indium for electrocatalytic Reduction of CO ₂ to Formic Acid. ChemCatChem, 2020, 12, 5632-5636.	3.7	13
79	Design of BiOBr0.25I0.75 for synergy photoreduction Cr(VI) and capture Cr(III) over wide pH range. Chinese Chemical Letters, 2022, 33, 3053-3060.	9.0	13
80	Coexistence of Magnetism and Ferroelectricity in 3d Transition-Metal-Doped SnTe Monolayer. Journal of Physical Chemistry C, 2019, 123, 28919-28924.	3.1	12
81	Band structure and optical properties of MoS2/SnO2 hetero-bilayer from hybrid functional calculations. Materials Chemistry and Physics, 2020, 239, 122071.	4.0	11
82	Large Interlayer Spacing of Few-Layered Cobalt–Tin-Based Sulfide Providing Superior Sodium Storage. ACS Applied Materials & Interfaces, 2020, 12, 41546-41556.	8.0	11
83	Efficient electrochemical water oxidation to hydrogen peroxide over intrinsic carbon defect-rich carbon nanofibers. Journal of Materials Chemistry A, 2021, 9, 23994-24001.	10.3	11
84	Hollow core-shell Z-scheme heterojunction on self-floating carbon fiber cloth with robust photocatalytic-photothermal performance. Journal of Cleaner Production, 2022, 360, 132166.	9.3	11
85	Activated edge of single layered TiO2 nanoribbons through transition metal doping and strain approaches for hydrogen production. Applied Surface Science, 2021, 545, 148947.	6.1	10
86	Synthesis of a Boron–Imidazolate Framework Nanosheet with Dimer Copper Units for CO 2 Electroreduction to Ethylene. Angewandte Chemie, 2021, 133, 16823-16828.	2.0	10
87	Transition-metal hydroxide nanosheets with peculiar double-layer structures as efficient electrocatalysts. Chem Catalysis, 2022, 2, 867-882.	6.1	10
88	Unveiling the Origin of Catalytic Sites of Pt Nanoparticles Decorated on Oxygen-Deficient Vanadium-Doped Cobalt Hydroxide Nanosheet for Hybrid Sodium–Air Batteries. ACS Applied Energy Materials, 2020, 3, 7464-7473.	5.1	9
89	Regulating the surface state of ZnIn ₂ S ₄ by gamma-ray irradiation for enhanced photocatalytic hydrogen evolution. Catalysis Science and Technology, 2022, 12, 927-934.	4.1	9
90	Prediction of functionalized graphene as potential catalysts for overall water splitting. Applied Surface Science, 2022, 578, 151989.	6.1	8

#	Article	IF	CITATIONS
91	Pt–Ni Alloy Nanoparticles via High-Temperature Shock as Efficient Electrocatalysts in the Oxygen Reduction Reaction. ACS Applied Nano Materials, 2022, 5, 8243-8250.	5.0	8
92	Tuning the ferromagnetism of a single layered titanium dioxide nanosheet with hole doping and uniaxial strain. Journal of Physics Condensed Matter, 2018, 30, 305804.	1.8	6
93	Electronic and Optical Properties of TiO ₂ Solid-Solution Nanosheets for Bandgap Engineering: A Hybrid Functional Study. Journal of Physical Chemistry C, 2017, 121, 18683-18691. First-principles study of the quasi-one-dimensional organic-inorganic hybrid perovskites <mml:math< td=""><td>3.1</td><td>5</td></mml:math<>	3.1	5

xmlns:mml="http://www.w3.org/1998/Math/MathML"> <mml:mrow> <mml:mrow> <mml:mo> (</mml:mo> <mml:mi>MV</mml:mi> <mml:mi> <mml:mi> </mml:mo> </mml:mi> Cl</mml:mi> <mml:mn>2 </mml:mn> </mml:mo> </mml:mi> <mml:mi> <mml:mi> </mml:mo> </mml:mo> </mml:mo> </mml:mi> </mml:mo> </ml>